Table 1. Cardiac hemodynamics with progression of HF

Strain	Age, weeks	LVP, mmHg	dP/dt_{max}, mmHg/sec	dP/dt_{min}, mmHg/sec	EDP, mmHg	CVP, mmHg
F_1B	5	82.9 ± 1.2	4,385 ± 91	−4,503 ± 208	3.1 ± 0.6	1.70 ± 0.53
	15	132.9 ± 5.5†	8,188 ± 743†	−7,188 ± 971†	1.8 ± 1.5	0.78 ± 0.50
	25	132.5 ± 6.9	6,709 ± 188	−6,513 ± 602	1.7 ± 2.7	0.46 ± 0.21
	40	125.1 ± 9.6	7,063 ± 290	−7,180 ± 576	1.6 ± 0.9	−0.62 ± 0.32
TO-2	5	83.0 ± 2.1	4,599 ± 192	−5,175 ± 233*	1.9 ± 0.3*	2.82 ± 0.17*
	15	100.2 ± 4.7*†	4,645 ± 637*	−3,664 ± 378*†	8.8 ± 1.9*†	2.70 ± 0.87*
	25	87.9 ± 8.3*	5,240 ± 388*	−3,171 ± 80*	12.8 ± 1.6*	3.12 ± 0.88*
	40	80.0 ± 2.8*	4,283 ± 97*	−3,120 ± 145*	18.0 ± 1.4*†	9.35 ± 1.35*†

Hemodynamic indices measured under stable anesthesia (7, 8): LVP, its maximum derivative (dP/dt_{max}) and minimum derivative (dP/dt_{min}), EDP, and CVP, in control (F_1B strain) and hereditary DCM (TO-2 strain) hamsters. Each value is shown as the mean ± SE (n = 4–8 hamsters in each group). * and † indicate statistical significance ($P < 0.05$) compared with the F_1B strain and the preceding age, respectively.

Hemodynamic Studies and Statistical Analyses. Peak left ventricular pressure (LVP), left ventricular end diastolic pressure (EDP), its first derivative (dP/dt), and central venous pressure (CVP) were measured under stable anesthesia (7, 8). All values were expressed as the mean ± SE and evaluated by paired Student's t test, ANOVA, and correlation analyses. A P value of <0.05 was considered significant.

Results and Discussion

Progression of DCM to Advanced HF in TO-2 Hamsters. Control F_1B hamsters showed growth-dependent increases in the peak LVP, the maximum rate of LVP (dP/dt_{max}), and the minimum rate of LVP (dP/dt_{min}, Table 1). In contrast, TO-2 hamsters persistently demonstrated systolic failure characterized by reduced LVP, dP/dt_{max}, and blunted dP/dt_{min}. Congestive HF was documented by increased left ventricular EDP and CVP. These signs became aggravated between 25 and 40 weeks of age, when the rate of cardiac death sharply increased (see below). The EDP and CVP reached levels 9.5 and 3.3 times higher, respectively, than those at 5 weeks of age.

Translocation of Dys from the SL to the Myoplasm During DCM Progression. Cardiac samples from TO-2 hamsters revealed time-dependent pathological features at each age (Fig. 1). After 5 weeks, double fluoromicroscopy showed that Dys was neatly arranged on the SL, and EB administered *i.v.* before killing the animals did not enter the myoplasm, indicating that the integrity of the SL was well preserved. After 25 and 40 weeks, the Dys on the SL became blurred, and some cardiomyocytes demonstrated a shift of Dys from the SL to the myoplasm. We refer to this phenomenon as "translocation" of Dys. These cardiomyocytes matched exactly with cells that took up EB (within ovals), denoting that the SL of the translocated cells leaked the exogenously applied dye.

Cleavage of Dys in Hamster Heart and in the Hearts of Humans with DCM. Western blotting of the myocardial homogenate with an antibody specific to the rod domain of Dys showed characteristic features (Fig. 2*a Left*). Normal hearts at 5 weeks of age showed a band at 430 kDa corresponding to normal Dys, and the staining intensity was preserved up to 40 weeks of age. Striking differences were observed in TO-2 hamsters, although at 5 and 15 weeks of age the staining pattern did not differ from that of the F_1B heart. However, at 25 weeks of age, extra bands were detected between 60 and 200 kDa (Fig. 2*a Left*), and the intensity of the Dys 430-kDa band started to decline. The intensity of this band was markedly reduced between 25 and 40 weeks of age, whereas the intensity of the 60-kDa band increased, mirroring the Dys band (Fig. 2*b*). The period of significant Dys cleavage matched exactly the periods when Dys translocation became

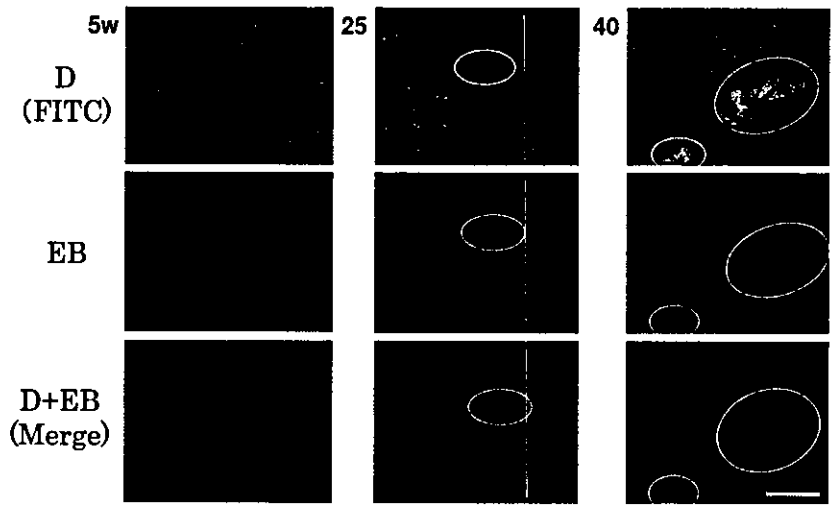

Fig. 1. Age-dependent translocation of Dys and increased permeability of the SL during HF progression in TO-2 hamsters. Double fluoromicroscopy for detection of a FITC-labeled antibody to the rod domain of Dys and entry of membrane-impermeable, fluorescent EB, at 5, 25, and 40 weeks of age (w). Cardiomyocytes demonstrating a shift of Dys from the SL to the myoplasm are shown in ovals. (Bar = 40 μm.)

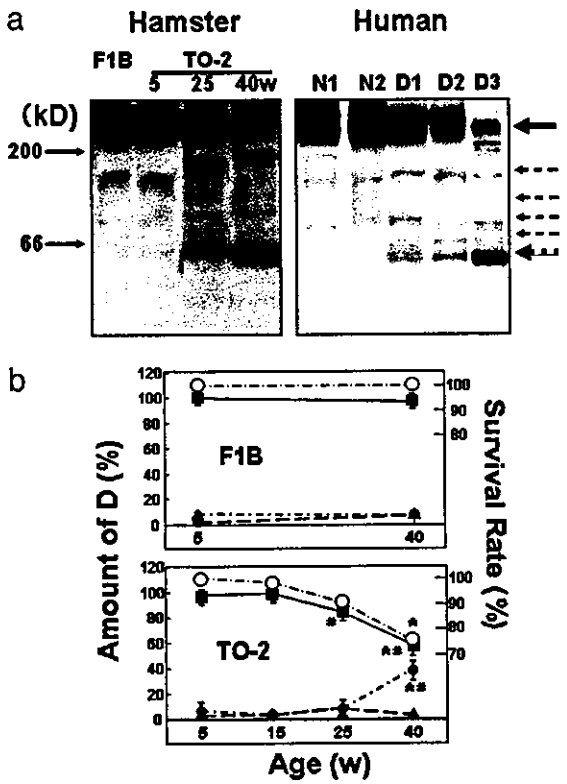

Fig. 2. Cleavage and reduction of cardiac Dys during DCM progression in hamsters and humans. (*a Left*) Control (F_1B strain) or DCM (TO-2 strain) hamsters at 5, 25, and 40 weeks of age (w). (*a Right*) Normal human myocardium (N1 and N2) and DCM hearts (D1, D2, and D3) at the time of cardiac transplantation. A solid arrow at 430 kDa and several dotted arrows denote the original Dys and its degradation products, respectively, after 5–20% SDS/PAGE of whole-heart homogenates. (*b*) Time course of the survival rate of control (F_1B; *Upper*) or DCM (TO-2; *Lower*) hamsters (○) and the density of immunoreactive bands specific to the rod domain of Dys at 430 (■), 60 (●) or 160 (▲) kDa. * and # indicate a significant difference, compared with the control F_1B strain and the preceding age, respectively.

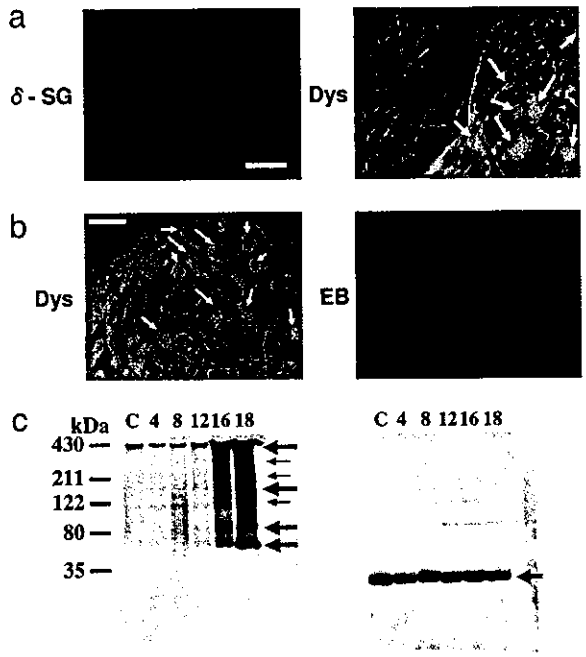

Fig. 3. (*a*) Double immunostaining of δ-SG (rhodamine isothiocyanate) and Dys (FITC) of TO-2 hamster hearts 35 weeks after local δ-SG gene transfection *in vivo* (8). Arrows indicate cardiomyocytes where dystrophin was translocated from the SL to the myoplasm. (Bar = 40 μm.) (*b*) Assessment of Dys translocation (FITC) and SL fragility *in situ* (EB entry) 16 h after the administration of Isp at a high dose (10 mg/kg i.p.) in Wistar rats (15). Arrows indicate cardiomyocytes where dystrophin was translocated from the SL to the myoplasm. (Bar = 40 μm.) (*c*) Western blotting of Dys (*Left*) and δ-SG (*Right*) from the same rat heart homogenate sample after gradient 10–15% SDS/PAGE of the control (C) and 4, 8, 12, 16 and 18 h after Isp treatment. Arrows indicate uncleaved Dys (430 kDa) and Dys degradation products (*Left*) or δ-SG (*Right*).

evident (Fig. 1) and when the animals started to die of congestive HF (ref. 8 and Fig. 2*b*). The intensity of the faint 160-kDa band did not change throughout the study and appeared to be unrelated to the progression of HF.

Similar cleavage of Dys was confirmed in hearts from patients with DCM of unidentified etiology who had undergone cardiac transplantation (Fig. 2*a Right*). The topological shift of Dys was also documented in samples of advanced stage DCM (unpublished data). Accordingly, the translocation was common to both animal models and patients with DCM. Other antibodies to the C or N terminus of Dys did not clearly recognize the cleavage product (data not shown). At present, we do not know the reason for this discrepancy in human cases of advanced HF showing selective cleavage of Dys at the N terminus (10).

Relationship of Dys Cleavage to Hemodynamics and the Lifespan of Hamsters. Surprisingly, the amount of Dys or its 60-kDa-band degradation product in TO-2 animals very closely correlated with the hemodynamic indices that characterize the progression of HF. The Dys amount was positively correlated with the systolic index [peak LVP, coefficient of regression (r) = 0.998 and $P < 0.0004$], and negatively correlated with the diastolic parameters (EDP, $r = 0.996$ and $P < 0.0005$; CVP, $r = 0.954$ and $P < 0.002$). The intensity of the 60-kDa band showed a clear negative correlation with the LVP ($r = 0.961$, $P < 0.002$) and a positive correlation with the EDP ($r = 0.954$, $P < 0.002$) and CVP ($r = 0.996$, $P < 0.0005$). These highly significant regression coefficients for correlation of the amount of Dys with systolic or diastolic performance support a tentative role for Dys in transmitting an effect through the actin–myosin linkage to the extracellular matrix. It is also noteworthy that no correlation was found between the amounts of Dys or the 60-kDa band and the dP/dt_{max} or dP/dt_{min} value (data not shown), both of which are regulated by Ca^{2+} handling (11) and the energetics of cardiac muscle cells (12). It should be emphasized that a distinct relationship was found between the amount of Dys or the 60-kDa band and the survival rate of the TO-2 animals over time (Fig. 2*b Lower*). It is possible that these immunological and hemodynamic data could be biased, because ≈30% of the TO-2 hamsters died of HF (Fig. 2*b Lower*), and we could only use the survivors in the analysis.

Effect of Long-Lasting Gene Therapy on Dys Localization. The final evidence that the disruption of Dys is not an epiphenomenon in HF but is actually caused by a loss of δ-SG is provided by the double immunostaining of Dys and δ-SG in TO-2 hearts with or without local gene transfection *in vivo* (Fig. 3*a*). In control F_1B hearts, both proteins were equally expressed on the SL (data not shown). In contrast, the TO-2 heart did not express δ-SG (13). As described above (Fig. 1), Dys staining became blurred with age, and some cardiomyocytes revealed Dys translocation (14). Gene delivery of normal δ-SG *in vivo*, by means of a nonpathogenic and long-lasting rAAV vector (7, 8), was used to locally express the δ-SG transgene, and this gene therapy completely ameliorated Dys translocation in the same cardiomyocytes for up to 35 weeks (Fig. 3*a Left*). In contrast, nontransfected cells

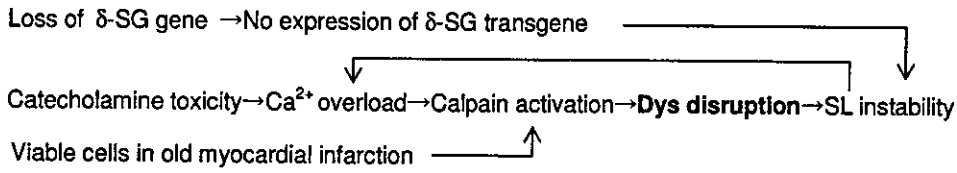

Scheme 1. Pathways for the progression of HF to an advanced stage.

showed translocation of Dys in the same sample (indicated by arrows in Fig. 3*a Right*). This finding specifically eliminates the possibility that Dys disruption resulted from the parallel development of HF, because Dys translocation was restricted to cardiomyocytes that did not express the δ-SG transgene. Furthermore, the amount of Dys estimated *in situ* by densitometry of immunofluoromicroscopic images in cardiomyocytes indicated a 1.22 ± 0.13 fold ($P < 0.01$) preferential localization of Dys on the SL of δ-SG-transfected cells ($n = 70$ cells per group).

Effect of Isp on SL Permeability, and Shift and Cleavage of Dys and δ-SG. A toxic dose of Isp (10 mg/kg i.p.) causes acute HF and morphological deterioration in normal rats (9). Pathological examination has shown time-dependent degradation of Dys and apoptosis of cardiomyocytes from 4 to 18 h after Isp was administered (15). Confocal microscopy of cardiomyocytes in the same observation field showed translocation of Dys (indicated by arrows in Fig. 3*b Left*) and entry of the SL-impermeable EB into the myoplasm of cardiac muscle cells. The shift of Dys was selectively detected 16 h after Isp treatment only in cardiomyocytes where EB had entered the myoplasm (Fig. 3*b Right*). Western blotting revealed time-dependent cleavage of Dys, showing degradation fragments between 60 and 200 kDa (Fig. 3*c Left*). In contrast, δ-SG was not hydrolyzed at all (Fig. 3*c Right*). Immunohistology confirmed that δ-SG did not shift from the SL but remained localized on the SL (data not shown). The effect of high-dose Isp, a β-adrenergic agonist, was similar to that observed in a DCM mouse with a protein kinase A knock-in gene (16). To verify the therapeutic effect of gene therapy in a β-adrenergic agonist/protein kinase A/phospholamban system, the pharmacological action (17, 18) and the disease prognosis need to be precisely examined, because an improvement in hemodynamics does not always prolong the lifespan of the animal (19).

The limited hydrolysis of Dys, common to the models of acute and chronic diseases in the present study, suggests a role for calpain, because cardiomyocytes contain an appreciable amount of this protein (20), and intracellular Ca^{2+} handling is modified in failing hearts (21, 22). Neither a specific inhibitor for calpain nor a calpain knockout animal is currently available to test this hypothesis. β-Adrenergic agonists induce Ca^{2+} overload in cardiomyocytes by increasing Ca^{2+} uptake (23). In addition, Dys and α-, β-, and γ-SG, but not δ-SG, are hydrolyzed by the endogenous protease (24) or isolated calpain *in vitro* (25, 26). The preferential breakdown of these proteins, but not δ-SG, in three HF models, i.e., TO-2 hamster hearts (13), Isp-treated rat hearts (Fig. 3*b*), and viable cells at the end stage of myocardial infarction (26), might be accompanied by substantially enhanced activity of *m*-calpain over its endogenous inhibitor, calpastatin. The expression of *m*-calpain in TO-2 hearts markedly exceeded that of calpastatin during the progression of HF (data not shown). These results may imply that the balance between calpain and calpastatin will shift in a calpain-dominant manner. Furthermore, dot hybridization analyses revealed no increment of mRNA of each DAP component under these HF conditions, suggesting that compensatory biosynthesis did not occur in the case of DAP.

A Scheme for the Progression of HF to an Advanced Stage. The clinical link between excess stimulation with catecholamines and myocardial damage has been confirmed by the therapeutic success of β-adrenergic antagonists in TO-2 hamsters (27) and humans (28, 29). The cleavage of Dys has also been documented after enterovirus infection, resulting in DCM-like HF (30). These pathological findings present a paradigm in which cardioselective cleavage of Dys may lead to progression of HF to an advanced stage (Scheme 1). Scheme 1 does not exclude the involvement of a protease cascade, as seen through the activation of a calpain-like homologue in neuronal degeneration in *Caenorhabditis elegans* (31), or involvement of the ubiquitin/proteasome system (32) in the loss of Dys. More definite evidence is required to precisely determine the causative factor(s). This common pathological process, irrespective of the hereditary or acquired origin and the chronic or acute course of the disease, suggests a strategy for the treatment of advanced HF through interruption of the vicious circle by either gene therapy or drug treatment.

We thank Dr. John R. Solaro (Department of Physiology and Biophysics, University of Illinois, Chicago) for discussion of the results and Dr. Y. Niwa and K. Kurosawa (Department of Pathophysiology, University of Tokyo) for experimental and secretarial assistance. This work was supported by Ministry of Education, Culture, and Science Grant A2 142070333 and by the Ministry of Welfare and Labor, Japan, the Mitsubishi Research Foundation, and the Motor Vehicle Foundation.

1. Cox, G. F. & Kunkel, L. M. (1997) *Curr. Opin. Cardiol.* **12**, 329–343.
2. Seidman, J. G. & Seidman, C. (2001) *Cell* **104**, 557–567.
3. Durbeej, M. & Campbell, K. P. (2002) *Curr. Opin. Genet. Dev.* **12**, 349–361.
4. Sakamoto, A., Ono, K., Abe, M., Jasmin, G., Eki, T., Murakami, Y., Masaki, T., Toyo-oka, T. & Hanaoka, F. (1997) *Proc. Natl. Acad. Sci. USA* **94**, 13873–13878.
5. Nigro, V., Okazaki, Y., Belsito, A., Piluso, G., Matsuda, Y., Politano, L., Nigro, G., Ventura, C., Abbondanza, C., Molinari, A. M., *et al.* (1997) *Hum. Mol. Genet.* **6**, 601–607.
6. Tsubata, S., Bowles, K. R., Vatta, M., Zintz, C., Titus, J., Muhonen, L., Bowles, N. E. & Towbin, J. A. (2000) *J. Clin. Invest.* **106**, 655–662.
7. Kawada, T., Sakamoto, A., Nakazawa, M., Urabe, M., Masuda, F., Hemmi, C., Wang, Y., Shin, W. S., Nakatsuru, Y., Sato, H., *et al.* (2001) *Biochem. Biophys. Res. Commun.* **284**, 431–435.
8. Kawada, T., Nakazawa, M., Nakauchi, S., Yamazaki, K., Shimamoto, R., Urabe, M., Nakata, J., Masui, F., Nakajima, T., Suzuki, J., *et al.* (2002) *Proc. Natl. Acad. Sci. USA* **99**, 901–906.
9. Kahn, D. S., Rona, G. & Chappel, C. I. (1969) *Ann. N.Y. Acad. Sci.* **156**, 285–293.
10. Vatta, M., Stetson, S. J., Perez-Verdia, A., Entman, M. L., Noon, G. P., Torre-Amione, G., Bowles, N. E. & Towbin, J. A. (2002) *Lancet* **359**, 936–941.
11. Ebashi, S., Nonomura, Y., Toyo-oka, T. & Katayama, E. (1976) *Symp. Soc. Exp. Biol.* **30**, 349–360.
12. Toyo-oka, T., Nagayama, K., Suzuki, J. & Sugimoto, T. (1992) *Circulation* **86**, 295–301.
13. Kawada, T., Nakatsuru, Y., Sakamoto, A., Koizumi, T., Shin, W. S., Okai-Matsuo, Y., Suzuki, J., Uehara, Y., Nakazawa, M., Satoh, H., *et al.* (1999) *FEBS Lett.* **458**, 405–408.
14. Kawada, T., Hemmi, C., Fukuda, S., Iwasawa, K., Tezuka, A., Nakazawa, M., Sato, H. & Toyo-oka, T. (2004) *Exp. Clin. Cardiol.* **8**, in press.
15. Xi, H., Shin, W. S., Suzuki, J., Nakajima, T., Kawada, T., Uehara, Y., Nakazawa, M. & Toyo-oka, T. (2000) *J. Cardiovasc. Pharmacol.* **36**, Suppl. 2, S25–S29.
16. Antos, C. L., Frey, N., Marx, S. O., Reiken, S., Gaburjakova, M., Richardson, J. A., Marks, A. R. & Olson, E. N. (2001) *Circ. Res.* **89**, 997–1004.

17. Bristow, M. R. (2001) *Circulation* **103,** 787–788.
18. Hoshijima, M., Ikeda, Y., Iwanaga, Y., Minamisawa, S., Date, M. O., Gu, Y., Iwatate, M., Li, M., Wang, L., Wilson, J. M., *et al.* (2002) *Nat. Med.* **8,** 864–871.
19. Jessup, M. & Brozena, S. (2003) *N. Engl. J. Med.* **348,** 2007–2018.
20. Toyo-oka, T., Shimizu, T. & Masaki, T. (1978) *Biochem. Biophys. Res. Commun.* **82,** 484–491.
21. Gwathmey, J. K., Copelas, L., MacKinnon, R., Schoen, F. J., Feldman, M. D., Grossman, W. & Morgan, J. P. (1987) *Circ. Res.* **61,** 70–76.
22. Whitmer, J. T., Kumar, P. & Solaro, R. J. (1988) *Circ. Res.* **62,** 81–85.
23. Naylor, W. G., Mas-Oliva, J. & Williams, A. J. (1980) *Circ. Res.* **46,** Part 2, 161–166.
24. Koenig, M. & Kunkel, L. M. (1990) *J. Biol. Chem.* **265,** 4560–4566.
25. Yoshida, M., Suzuki, A., Shimizu, T. & Ozawa, E. (1992) *J. Biochem.* **112,** 433–439.
26. Yoshida, H., Takahashi, M., Koshimizu, M., Tanonaka, K., Oikawa, R., Toyo-oka, T. & Takeo, S. (2003) *Cardiovasc. Res.* **59,** 419–427.
27. Opie, L. H., Walpoth, B. & Barsacchi, R. (1985) *J. Mol. Cell. Cardiol.* **17,** Suppl. 2, 21–34.
28. Gottlieb, S. S., McCarter, R. J. & Vogel, R. A. (1998) *N. Engl. J. Med.* **339,** 489–497.
29. Packer, M., Coats, A. J., Fowler, M. B., Katus, H. A., Krum, H., Mohacsi, P., Rouleau, J. L., Tendera, M., Castaigne, A., Roecker, E. B., *et al.* (2001) *N. Engl. J. Med.* **344,** 1651–1658.
30. Badorff, C., Lee, G. H., Lamphear, B. J., Martone, M. E., Campbell, K. P., Rhoads, R. E. & Knowlton, K. U. (1999) *Nat. Med.* **5,** 320–326.
31. Syntichaki, P., Xu, K., Driscoll, M. & Tavernarakis, N. (2002) *Nature* **419,** 939–944.
32. Bonuccelli, G., Sotgia, F., Schubert, W., Park, D. S., Frank, P. G., Woodman, S. E., Insabato, L., Cammer, M., Minetti, C. & Lisanti, M. P. (2003) *Am. J. Pathol.* **163,** 1663–1675.

RESEARCH

Separate Control of Rep and Cap Expression Using Mutant and Wild-Type LoxP Sequences and Improved Packaging System for Adeno-Associated Virus Vector Production

*Hiroaki Mizukami, Takashi Okada, Yoji Ogasawara, Takashi Matsushita, Masashi Urabe, Akihiro Kume, and Keiya Ozawa**

Abstract

Adeno-associated virus (AAV) vectors are a practical choice for gene transfer, and demand for them is increasing. To cope with the necessity in the near future, we have developed a number of approaches to establish packaging cell lines for the production of AAV vectors. In our previous study, a highly regulated expression of large Rep proteins was obtained by using the Cre–loxP switching system. Therefore, in the present study, to regulate Cap expression as well, we developed an inducible expression system for both Rep and Cap proteins by using an additional set of mutant loxP sequences. The mutants possess two base alterations in the spacer region of loxP and recombine specifically with the same counterpart in the presence of Cre. By using two separate plasmids, one with mutant and the other with wild-type loxP sequences, the expression of two different proteins can be induced simultaneously by Cre recombinase. When the LacZ-encoding plasmid vector was used as a packaging model, a significant packaging titer of 2.1×10^{10} genome copies per 10-cm dish was obtained. These results indicate the importance of controlling Cap expression, in addition to Rep, to achieve an optimum production rate for AAV vectors.

Index Entries: Cre–loxP; mutant loxP; dependovirus; AAV vector; packaging cell line; 293 cells.

1. Introduction

Adeno-associated viruses (AAVs) are currently being investigated as a gene transfer vector for a variety of applications. Several diseases are thought to be prime candidates for AAV vector-medicated therapeutic intervention; clinical trials are already set out for the correction of hemophilia B *(1)*, and for Parkinson's disease in the near future *(2,3)*. However, one drawback to the use of AAV is difficulty in making large-scale preparations. To improve the process of preparation, we have developed packaging cell lines for AAV *(4,5)*. Early studies indicate that in addition to Rep, relatively large amounts of Cap proteins should be expressed to achieve a high titer of virus production, despite the fact that constitutive expression of these proteins has cytotoxic consequences *(6,7)*. Therefore, controlling the expression profiles for these proteins has vital significance. For this purpose, the Cre–loxP system is one of the best-known approaches as an induction system, and in our previous study we used loxP sequences to regulate Rep expression *(4)*. However, there was a limitation to this approach in that Cap expression could not be regulated efficiently; only Rep expression could be regulated. To control Cap expression in addition to Rep expression, we used mutant loxP sequences along with the wild type. These mutant loxP sequences are shown to recombine specifically with each

*Author to whom all correspondence and reprint requests should be addressed: Dr. Keiya Ozawa, Division of Genetic Therapeutics, Center for Molecular Medicine, Jichi Medical School, 3311-1, Yakushiji, Minamikawachi-machi, Kawachi-gun, Tochigi, 329-0498, Japan.E-mail: kozawa@ms2.jichi.ac.jp

other, but less efficiently with wild-type sequences on treatment with Cre *(8)*. In the present study, we compared the efficiency of recombination and designed plasmids to express optimal amounts of Rep and Cap proteins on Cre treatment. By optimizing these parameters, we developed a packaging cell line with improved production rate compared with our prototype cell line.

2. Materials and Methods

2.1. Cells and Plasmids

A human embryonic kidney cell line, known as 293 cells *(9)*, was maintained as described previously *(4)*. Plasmid ploxlox (a gift from Dr. Jamey D. Marth), which contains two adjacent loxP sequences in the same direction, was used as a backbone for the wild-type loxP *(10)*. To make plas-mids with mutant loxP, the sequences corresponding to the spacer region of loxP were mutated by synthesizing oligonucleotides based on published sequence information (**Fig. 1A**) *(8)*. Briefly, the spacer region of wild-type loxP constitutes ATGTATGC; for the loxP (V) and loxP(S), the sequences correspond to 5'-ATGT GTAC-3' and 5'-AAGTATCC-3', respectively. The CAG promoter (a gift from Dr. J Miyazaki, Osaka University, Japan) *(11)*, neomycin resistance gene, blasticidin S resistance gene (Invitrogen Corp., Carlsbad, CA), bacterial LacZ sequence, and AAV sequences corresponding to *p5*, *rep*, and *cap* genes were excised and ligated to complete plasmids named CAPBPL, CAVBVL, CASBSL, CAPBPC, and p5SNSR, respectively (*see* **Fig. 1B**), using standard techniques as reported previously *(4)*.

2.2. Induction of Recombination and Demonstration of Gene Expression

Plasmids encoding *LacZ* gene with the "stuffer" sequences between the two loxP sequences (CAPBPL, CAVBVL, CASBSL) were introduced into 293 cells using a standard calcium phosphate transfection technique *(12)*. Briefly, 1 μg of plasmid was mixed with 150 μL of 0.3*M* $CaCl_2$ and 2X HBS buffer and added to a single 6-well chamber. Six hours later, the medium was replenished. To assess the efficiency of recombination, a Cre-expressing adenovirus vector (AxCANCre, a gift from Dr. I. Saito) was applied to the culture thereafter at an MOI of 1 *(13)*. At various time-points, cells were dislodged, lysed, and β-galactosidase activity was measured by orthonitrophenyl-β-galactosidase assay (Invitrogen Corp., Carlsbad, CA) according to the manufacturer's instructions. Lysates were then subjected to Western analyses, either with anti-Rep (clone 303.9, Progen, Heidelberg, Germany) or anti-Cap (clone B1, Progen, Heidelberg, Germany), as reported previously *(4)*.

2.3. Development of Clones

Seven micrograms of each plasmid were used to transfect one 10-cm dish of 293 cells using a standard calcium-phosphate method at 70% of confluence. Forty-eight hours later, the cells were replated to several dishes and exposed to the selection medium containing both 800 μg/mL of G418 and 10 μg/mL of blasticidin S. The selection medium was replenished every 3 d. After 2 to 3 wk of selection, individual clones were recovered and amplified in 12-well plates in the presence of a half concentration of the selection medium of G418 and Blasticidin S. When a clone grew to semiconfluence in a 12-well plate, it was assumed to be established and was subjected to the analysis for packaging titer. The clones were numbered according to the order of establishment.

2.4. Titration of Vector Production

Established clones were further expanded, replated in new 12-well plates, then transfected with 0.5μg of the vector plasmid containing the *LacZ* gene cassette (driven by cytomegalovirus [CMV] promoter) flanked by two ITR sequences. Six hours after transfection, the medium was replenished, and Cre-expressing adenoviruses (AxCANCre) were added at an MOI of 1. Forty-eight hours later, cells were collected, subjected to three cycles of freeze–thawing, and treated with deoxyribonuclease I (Takara Bio, Inc., Ohtsu, Japan) for 30 min at 370°C as indicated by the manufacturer. The samples were quantified using dot-blot analysis. Known copy numbers of LacZ-expressing plasmid was used as controls.

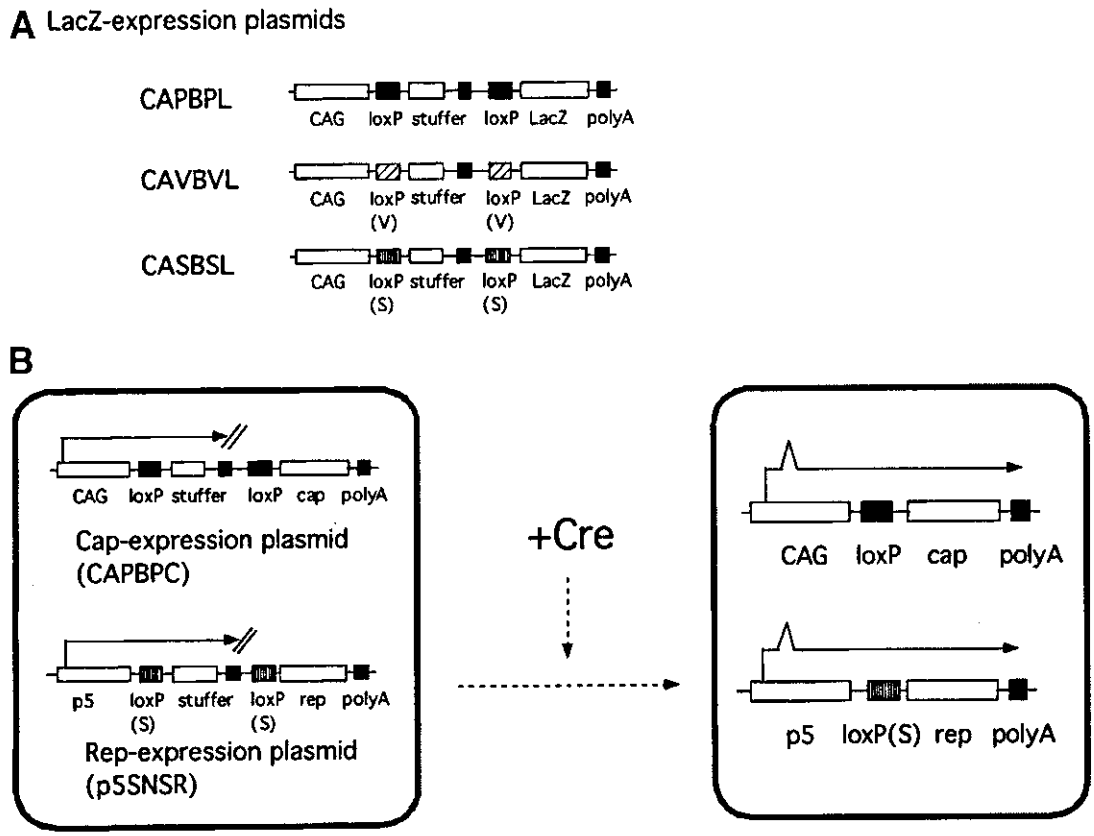

Fig. 1. Plasmid structure and the scheme of the cell line development. (**A**). To assess the recombination efficiency of the mutant loxP, three LacZ-expression plasmids are constructed. On infection with Ad-Cre, the stuffer sequences are removed with the efficiency depending on the wild-type or mutant loxP sequences, and the *LacZ* genes are driven by the CAG promoter. (**B**). The design of the cell line and the strategy for *rep* and *cap* expression are shown. To control *rep* and *cap* expression, a stuffer sequence is flanked by two loxP (wild-type or mutant) sequences. In the presence of Cre recombinase, the stuffer sequences are removed and the *cap* and *rep* genes are expressed.

2.5. Demonstration of Cre-Mediated Recombination by Polymerase Chain Reaction

Genomic deoxyribonucleic acid (DNA) was extracted from clone no. 3 by the standard techniques. Briefly, the recovered cells were treated with proteinase K, and total DNA was extracted with phenol chloroform. One microgram of total DNA was used as a template. A thermal cycler and the DNA polymerase ex-*Taq* (Takara Bio Inc., Ohtsu, Japan) were used for the PCR reaction according to the manufacturer's instructions. The forward primer sequences were 5'-TTC GGC TTC TGG CGT GTG AC-3' and 5'-TTG CGA CAT TTT GCG ACA CCA-3' for the *cap* and *rep* sequences, respectively. The reverse primer sequences were 5'-TCT GCG TAG TTG ATC GAA GCT-3' and 5'-GGG ACC TTA ATC ACA ATC TCG-3', respectively. The conditions for PCR were 940°C for 30 s, 560°C for 30 s, and 720°C for 1 min, and a total of 20 cycles of amplification were applied. The products were analyzed by agarose gel electrophoresis (0.8%) and visualized through ethidium bromide staining.

2.6. Statistical Analysis

The significance of the difference was estimated by Student's paired *t*-test.

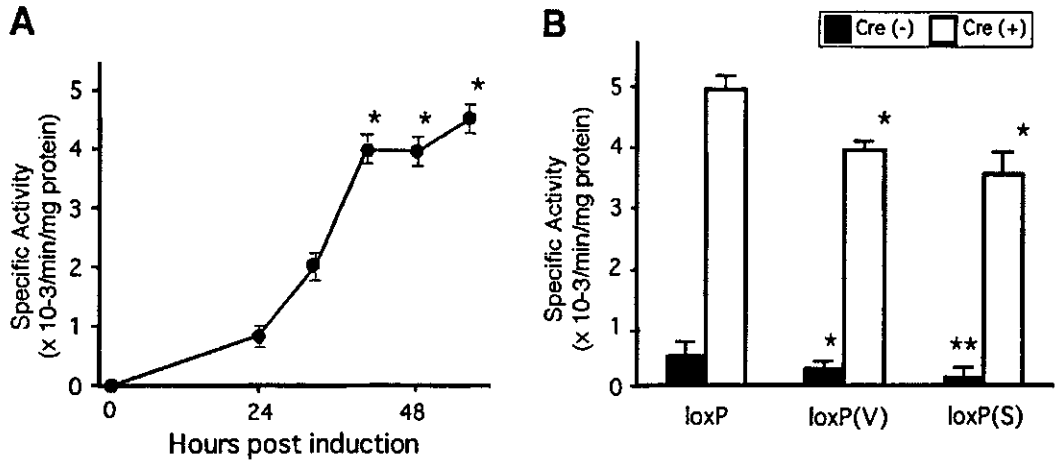

Fig. 2. Efficiency of recombination demonstrated in the wild-type and the mutant loxP. (**A**). Recombination activity of the wild-type loxP assessed at different time-points. The *asterisks* indicate the statistical significance ($p < 0.05$) of each data point against the nonindicated points. No significant differences were observed among the data points indicated by an asterisk. (**B**). Recombination efficiencies of wild-type and mutant loxP sequences. LacZ-expressing plasmids described in **Fig 1A** were used. Following transfection of the plasmids, 293 cells were infected by Ad-Cre at an MOI of 1. After 48 h, b-Gal activity was quantified. As for the baseline expression, values observed by loxP(V) were significantly lower than those with wild type as indicated by an *asterisk*. The baseline expression with loxP(S) was further significantly lower than that with loxP(V), as indicated by two *asterisks*. In terms of the expression levels following induction with Cre, values with both mutant loxPs showed significantly lower expression than those with wild type, as indicated by an *asterisk*. No differences were found in the values obtained by the mutant loxPs.

3. Results

3.1. Recombination Efficiency of Wild-Type and Mutant LoxP

To determine the optimal conditions for Cre–loxP-mediated induction of gene expression, we first examined the efficiency of recombination at various time-points. Recombination became significant at 40 h of induction by Ad-Cre and reached a plateau level thereafter (**Fig. 2A**). Therefore, we selected 48 h as a standard time-point for assessment of recombination. Then we compared the efficiency of recombination among the loxP sequences. The wild-type loxP showed the highest recombination efficiency, as assessed by LacZ expression (**Fig. 2B**). Therefore, we selected wild-type loxP for Cap expression plasmid. On the other hand, we selected the loxP (S) sequences for the Rep expression plasmids, as the basal level of expression was the lowest with this system.

3.2. Expression of Rep and Cap on Induction

Rep and Cap expression could be induced simultaneously by Cre recombinase (**Fig. 3**). Coexpression of the other protein inhibited the expression levels in both cases. The degree of Cap suppression was clearer than that of Rep suppression.

3.3. Development of Clones With Packaging Capacity

Following a period of 2–3 wk in selection medium containing both blasticidin S and G418, a total of 192 clones were chosen and amplified into 6-well culture plates. Of these, 22 clones reached semiconfluence in 10-cm dishes. These clones were further amplified, transfected with LacZ-expressing vector plasmids, and their ability to produce vector was determined. All of the 22 clones showed significant levels of vector production (**Table 1**). These LacZ-encoding vectors were capable of transducing 293 cells with similar effi-

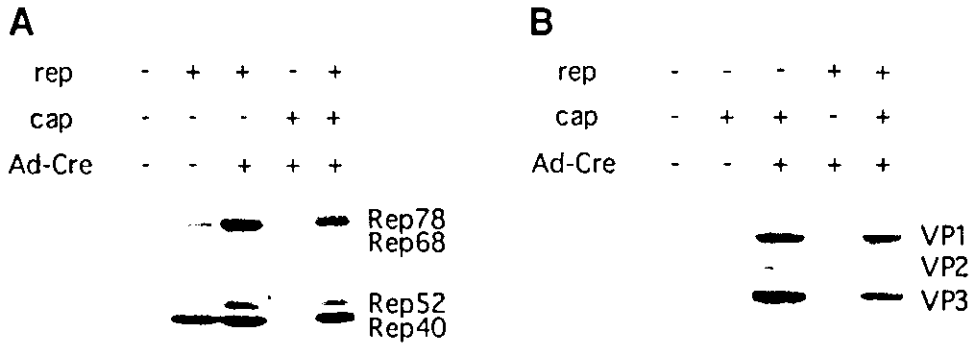

Fig. 3. *Rep* and *cap* expression profiles on treatment with Cre recombinase. One microgram of each plasmid was transfected into 293 cells in a 6-well plate. Following transfection, the cells received Ad-Cre and were lysed 48 h later. The cell lysates were analyzed by Western blotting using the monoclonal antibodies (**A**) 303.9 for *rep*, and (**B**) B1 for *cap*, respectively.

ciency to that made by the standard transfection method as assessed by conventional X-Gal staining (data not shown).

3.4. Stability of the Clones Developed

The established clones were further amplified and their stability was assessed at different time-points. As shown in **Table 1**, among the 22 clones developed, 6 continued to amplify for 2 wk. All of the expanded clones showed a significant packaging capacity. Of these, four clones tolerated additional expansion. These clones kept the growth speed of 293 cells, whereas the clones developed later (the higher numbered clones) tended to become slow growing. Of these, clone no. three maintained a significant packaging capacity throughout this period in terms of production of the AAV vector.

3.5. Detection of Cre-Mediated Recombination Events

Results of the analysis of clone no. 3 are shown in **Fig. 4**. PCR detection resulted in the amplification of the 1.1 and 1.2 kb for cap- and rep-expressing sequences within the untreated cells. Following Cre administration, shorter truncated sequences with 0.3 and 0.2 kb were amplified, suggesting simultaneous recombination events.

Table 1
The Actual Titer of the Clones Obtained in This Study

Clone no.	0 Wk[a]	2 Wk	4 Wk
3	20.9[b]	11.6	15.0
8	15.3	6.7	1.3
10	11.3	4.4	0.4
11	0.7	—	—
12	31.5	2.4	2.8
15	2.5	—	—
17	5.2	—	—
22	2.9	—	—
25	3.4	—	—
27	7.5	—	—
28	15.0	12.5	—
31	1.6	—	—
33	6.7	—	—
34	5.5	—	—
35	7.7	—	—
36	2.6	—	—
38	10.6	—	—
40	2.9	—	—
41	5.8	—	—
44	10.9	11.1	—
57	4.4	—	—
60	1.8	—	—

[a]The time-point started when a clone grew to semiconfluence within a 10-cm dish. At that time, the clone was challenged for packaging titer. Clone no. 3 retained a significant packaging capacity throughout the study.
[b]Titers of AAV vector per 10-cm dish ($\times 10^9$)

4. Discussion

In this study, we extended our previous findings *(4,5)* to regulate the expression of both *rep* and *cap* simultaneously, leading to development of a novel packaging cell line for the production of AAV vectors. Numerous attempts have been made to establish packaging cell lines, and sev-

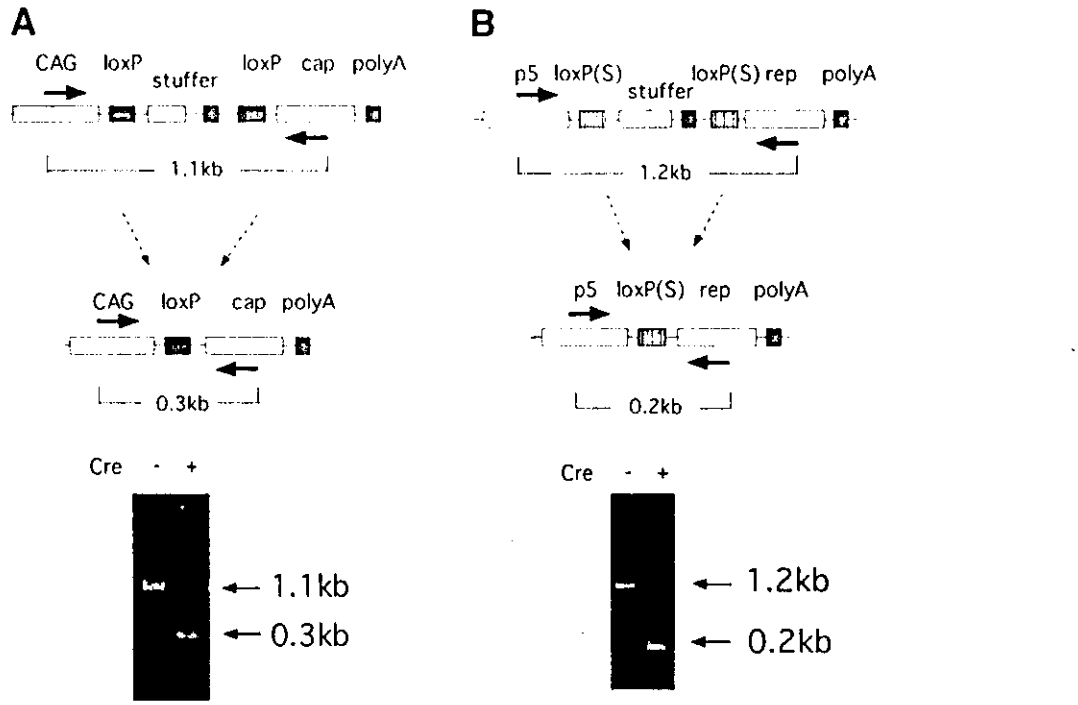

Fig. 4. The positions of the primers designed to detect both vector sequences before and after recombination are indicated by arrows. Primers corresponding to the CAG promoter and cap sequences or primers for p5 and *rep* sequences were used to amplify the vector sequences in (**A**) and (**B**), respectively. In both cases, a smaller number of cycles (20 cycles for this experiment) were used to avoid plateau-level amplifications.

eral promising lines with high production rates have been reported ***(14,15)***. Our strategy is advantageous in that there is a potential to optimize the condition for expressing Rep and Cap independently, as the genes of interest are encoded into two separate plasmids. In our previous study, we developed a cell line using Cre/loxP system to regulate Rep expression ***(4)***. Our present study showed that the simultaneous regulation of Cap expression in addition to Rep resulted in the improvement of production rate by 30-fold. The ideal amounts for the optimal production of vector are examined using two different plasmids encoding for *rep* and *cap* ***(16)*** by transient transfection, and the result indicates that a large amount of Cap and relatively small amount of Rep are suitable for the maximum production rate. To accomplish these conditions, we used a stronger promoter for *cap* and a weaker one for *rep*. Also, the choice of loxP sequences from a panel of mutant and wild-type sequences merits discussion in terms of recombination efficiency and leakage. Recombination efficiencies of the mutant and wild-type loxP in our system were comparable to those reported earlier ***(8)***. In addition to the recombination efficiency, the degree of "leakage" is also important to avoid toxicity, especially for Rep. As demonstrated in **Fig. 2B**, wild-type loxP showed the highest leakage despite the fact that it recombines most efficiently. As Rep proteins are highly toxic, the baseline expression must be kept as low as possible. Also, it is known that Rep expression need not be high even after induction. For these reasons, loxP (S) seemed to be the appropriate choice for the *rep*-expressing plasmids. Because low-level expression of Rep proteins is optimal for efficient vector production, a weak native promoter (p5) was used for the Rep-expression plasmid. On the other hand, because the expression of a large amount of Cap protein is required, a strong CAG

promoter was selected in combination with wild-type loxP sequences for the Cap-expression plasmid. CAG promoters have been shown to be strong and versatile in various systems *(17)*.

In **Fig. 3**, we observed a reduction in Rep or Cap expression in the presence of the other protein. Especially, Cap expression was suppressed by the presence of Rep. This may reflect the interference of both proteins, especially at the time of overexpression.

Although we tried to obtain a suitable condition for vector production, there is a possibility that the other factors might influence the optimal conditions. Of particular concern are the choice of producer cell type and promoters. For the prototype, we used 293 cells for a number of reasons. First of all, as 293 cells are derived from nonmalignant cells, they are appropriate for production of clinical-grade vectors. Also, we have several experiences developing cell lines based on 293 cells. The cells are easy to handle, and can be introduced efficiently into genes by conventional transfection methods. Regarding the promoter to drive *rep* and *cap* genes, there is a wide range of choice. Our use of heterologous promoters may contribute to high titers of vector production *(16)*.

The stability of the cells is also an important aspect from a practical point of view. In this study, we followed virus production for 4 wk after development. This period is sufficient for the cells in a large-scale culture. We numbered the clones according to the order of establishment. As a matter of fact, for the clones that developed later, there was a tendency not to survive long enough to assess their capability. Actually, clones later than no. 60 could not be expanded sufficiently to assess their long-term potential. Although the precise mechanisms are not clear, these properties in growth may be related to the leaky expression of Rep and Cap before induction with Cre. It is likely that only clones with optimum conditions can continue to grow during the course of large-scale expansion.

The use of AAV vectors is moving toward clinical applications. The refinement of the vector production system is vital to meet the anticipated increase in demand.

Acknowledgments

The authors are grateful to Drs. I. Saito and Y. Kanegae for valuable advice concerning mutant loxP sequences and for Cre-expressing adenovirus vectors. Also, we thank RIKEN DNA bank (Tsukuba, Japan) for distributing adenovirus vectors, and Avigen, Inc. for supplying plasmids for AAV vector production. This work was supported in part by grants from the Ministry of Health, Labor and Welfare of Japan and Grants-in Aid for Scientific Research from the Ministry of Education, Culture, Sports, Science and Technology.

References

1 Kay, M. A., Manno, C. S., Ragni, M. V., et al. (2000) Evidence for gene transfer and expression of factor IX in haemophilia B patients treated with an AAV vector. *Nat Genet.* **24,** 257–261.

2 During, M. J., Kaplitt, M. G., Stern, M. B., and Eidelberg, D. (2001) Subthalamic GAD gene transfer in Parkinson disease patients who are candidates for deep brain stimulation. *Hum. Gene Ther.* **12,** 1589–1591.

3 Muramatsu, S., Fujimoto, K., Ikeguchi, K., et al. (2002) Behavioral recovery in a primate model of Parkinson's disease by triple transduction of striatal cells with adeno-associated viral vectors expressing dopamine-synthesizing enzymes. *Hum. Gene Ther.* **13,** 345–354.

4 Ogasawara, Y., Mizukami, H., Urabe, M., et al. (1999) Highly regulated expression of adeno-associated virus large Rep proteins in stable 293 cell lines using the Cre/loxP switching system. *J. Gen. Virol.* **80,** 2477–2480.

5 Okada, T., Mizukami, H., Urabe, M., et al. (2001) Development and characterization of an antisense-mediated prepackaging cell line for adeno-associated virus vector production. *Biochem. Biophys. Res. Commun.* **288,** 62–68.

6 Holscher, C., Horer, M., Kleinschmidt, J. A., Zentgraf, H., Burkle, A., and Heilbronn, R. (1994) Cell lines inducibly expressing the adeno-associated virus (AAV) rep gene: requirements for productive replication of rep-negative AAV mutants. *J. Virol.* **68,** 7169–7177.

7 Yang, Q., Chen, F., and Trempe, J. P. (1994) Characterization of cell lines that inducibly express the adeno-associated virus Rep proteins. *J. Virol.* **68,** 4847–4856.

8 Lee, G. and Saito, I. (1998) Role of nucleotide sequences of loxP spacer region in Cre-mediated recombination. *Gene* **216,** 55–65.

9 Graham, F. L., Smiley, J., Russell, W. C., and Nairn, R. (1977) Characteristics of a human cell line trans-

formed by DNA from human adenovirus type 5. *J. Gen. Virol.* **36,** 59–74.

10 Orban, P. C., Chui, D., and Marth, J. D. (1992) Tissue- and site-specific DNA recombination of transgenic mice. *Proc. Natl. Acad. Sci. USA* **89,** 6861–6865.

11 Niwa, H., Yamamura, K., and Miyazaki, J. (1991) Efficient selection for high-expression transfectants with a novel eukaryotic vector. *Gene* **108,** 193–199.

12 Wigler, M., Pellicer, A., Silverstein, S., and Axel, R. (1978) Biochemical transfer of single-copy eukaryotic genes using total cellular DNA as a donor. *Cell* **14,** 725–731.

13 Kanegae, Y., Lee, G., Sato, Y., et al. (1995) Efficient gene activation in mammalian cells by using recombinant adenovirus expressing site-specific Cre recombinase. *Nucleic Acids Res.* **23,** 6816–3821.

14 Gao, G. P., Qu, G., Faust, L. Z., et al. (1998) High-titer adeno-associated viral vectors from a Rep/Cap cell line and hybrid shuttle virus. *Hum. Gene Ther.* **9,** 2353–2362.

15 Inoue, N. and Russell, D. W. (1998) Packaging cells based on inducible gene amplification for the production of adeno-associated virus vectors. *J. Virol.* **72,** 7024–7031.

16 Ogasawara, Y., Urabe, M., Kogure, K., et al. (1999) Efficient production of adeno-associated virus vectors using split-type helper plasmids. *Jpn. J. Cancer Res.* **90,** 476–483.

17. Kiwaki, K., Kanegae, Y., Saito, I., et al. (1996) Correction of ornithine transcarbamylase deficiency in adult spf(ash) mice and in OTC-deficient human hepatocytes with recombinant adenoviruses bearing the CAG promoter. *Hum. Gene Ther.* **7,** 821–830.

Journal of General Virology (2004), 85, 2209–2214 DOI 10.1099/vir.0.79940-0

Short Communication

The adenovirus E1A and E1B19K genes provide a helper function for transfection-based adeno-associated virus vector production

Takashi Matsushita,[1] Takashi Okada,[1] Toshiya Inaba,[2] Hiroaki Mizukami,[1] Keiya Ozawa[1] and Peter Colosi[3]

Correspondence
Takashi Okada
tokada@jichi.ac.jp
Peter Colosi
PColosi@avigen.com

[1]Division of Genetic Therapeutics, Center for Molecular Medicine, Jichi Medical School, 3311-1 Yakushiji, Minami-kawachi, Kawachi, Tochigi 329-0489, Japan

[2]Department of Molecular Oncology, Research Institute for Radiation Biology and Medicine, Hiroshima University, Hiroshima 734-8553, Japan

[3]Avigen Inc., Alameda, CA, USA

Although the adenoviral E1, E2A, E4 and VA RNA regions are required for efficient adeno-associated virus (AAV) vector production, the role that the individual E1 genes (*E1A*, *E1B19K*, *E1B55K* and *protein IX*) play in AAV vector production has not been clearly determined. E1 mutants were analysed for their ability to mediate AAV vector production in HeLa or KB cells, when cotransfected with plasmids encoding all other packaging functions. Disruption of *E1A* and *E1B19K* genes resulted in vector yield reduction by up to 10- and 100-fold, respectively, relative to the wild-type E1. Interruption of the *E1B55K* and *protein IX* genes had a modest effect on vector production. Interestingly, expression of anti-apoptotic E1B19K cellular homologues such as Bcl-2 or Bcl-x_L fully complemented E1B19K mutants for AAV vector production. These findings may be valuable for the future development of packaging cell lines for AAV vector production.

Received 26 December 2003
Accepted 17 May 2004

Adeno-associated virus (AAV)-based vector systems are particularly attractive vehicles for clinical applications requiring long-term *in vivo* gene expression from post-mitotic tissues. AAV vectors have been shown to promote stable expression of a wide variety of transgenes in numerous tissues, including skeletal and cardiac muscle, liver, the central nervous system and retina (Rabinowitz & Samulski, 1998). Overt evidence of inflammation is either minimal or non-existent in target tissues immediately following AAV vector administration. Furthermore, cytotoxic T-lymphocyte responses are not normally elicited to transgene products delivered by AAV vectors, even when such proteins are foreign to the host (Jooss *et al.*, 1998). AAV vectors are considered to be relatively safe because the parental virus is non-pathogenic and unable to replicate in the absence of a co-infecting helper virus. Additionally, current production methods have reduced the regeneration of replication competent wild-type AAV during vector production to undetectable levels (Allen *et al.*, 1997). Finally, the robust protein capsid of AAV makes AAV vectors particularly amenable to existing production methods for protein pharmaceuticals (Gao *et al.*, 2000) and confers upon them desirable drug stability characteristics.

AAV2, the parent virus from which the vector system is derived, is replication defective and requires co-infection of helper viruses to propagate. Adenovirus (Atchinson *et al.*, 1965) and herpes virus (Buller *et al.*, 1981) act as complete helpers and vaccinia virus (Schlehofer *et al.*, 1986) acts as a partial helper. The set of adenoviral (type 2 or 5) genes that facilitate AAV2 propagation has been defined and consists of E1A, E1B55K, the VA RNAs, E2A and E4orf6 (Samulski & Shenk, 1988). E1A acts as a cue to begin virus replication by up-regulating transcription from the *rep* gene promoters, P5 and P19 (Tratschin *et al.*, 1984) and by activating the early adenovirus promoters. E1A is also required to drive the host cell into the S-phase of the cell cycle for viral DNA replication because the AAV encoded proteins are not capable of this function. An adverse effect of E1A is that it stabilizes p53, which leads to apoptosis (Lowe *et al.*, 1993). To prevent this, the E1B55K and the E4orf6 proteins form a complex with p53 and cause it to be degraded through ubiquitin-mediated proteolysis (Querido *et al.*, 1997; Steegenga *et al.*, 1998). Later in infection, E1B55K and E4orf6 form a heterodimer that causes the preferential export of AAV and adenoviral late mRNAs from the nucleus while inhibiting the transit of adenoviral early and cellular mRNAs (Pilder *et al.*, 1986). The 72 kDa DNA-binding protein encoded by E2A has functions in viral DNA replication, viral mRNA processing and export, and AAV promoter regulation (Carter *et al.*, 1992; Ward *et al.*, 1998; Chang & Shenk, 1990). It causes an increase in the intracellular levels of the

single- and double-stranded forms of the AAV genome, the spliced forms of the rep proteins, and dramatically increases capsid protein production. Lastly, the VA RNAs inhibit the interferon-inducible eIF-2 protein kinase, thereby circumventing this cellular anti-viral mechanism from blocking viral protein translation (West *et al.*, 1987).

With respect to E2A, E4orf6 and the VA RNAs, the helper gene requirement for AAV vector and virus production is identical. We and others, have shown that plasmids encoding these genes, when cotransfected into 293 cells along with plasmids encoding rep/cap and a vector, mediate higher levels of vector production than that produced by adenovirus infection (Xiao *et al.*, 1998; Matsushita *et al.*, 1998). This so-called 'triple plasmid' transfection method forms the basis of the current scale-up vector production effort at Avigen and has a respectable mean production efficiency of 1×10^{13} vector genomes produced per 850 cm^2 roller bottle. A report was published describing a method for producing AAV vector in 293 cells using only E4orf6 as the helper gene (Allen *et al.*, 2000). This method requires the use of a heterologous promoter to drive the capsid gene and is about 10-fold less productive than methods using a plasmid encoding all three adenoviral helper genes (unpublished data).

The genes of the E1 region have not been analysed for their contribution to AAV vector production. In this study, we have investigated the role of the *E1A* and *E1B* genes in AAV vector production by using a series of E1 mutant plasmids and cell lines that lack adenoviral genes. E1A was required for efficient vector production. In contrast to the helper requirements for AAV production, our data indicated that *E1B19K* gene greatly augmented vector production, however, *E1B55K* gene did not.

The contributions of each of the component genes from the E1 region to AAV helper function was assessed by creating a set of plasmids with mutations in the *E1A*, *E1B19K*, *E1B55K* or *protein IX* genes and then testing them for their ability to support transfection-based AAV vector production. At least one truncation or one deletion mutation was made for each gene (Fig. 1).

For vector construction the plasmid pE1, which encodes the *E1A*, *E1B19K*, *E1B55K* and *protein IX* genes, was created from Ad2 DNA (Invitrogen). Briefly, the *Afl*III fragment (nt positions 142–5927) of Ad2 was cloned into the *Afl*III site of pBR322 (New England Biolabs) to generate pE1. pE1A-825stop was constructed by the insertion of an adapter (CCGGACTAATTAACTAGT), which includes a stop codon and an *Spe*I site, into the *Bsp*EI site of pE1. Similarly, pE1B19K-1912stop, pE1B55K-2243stop,

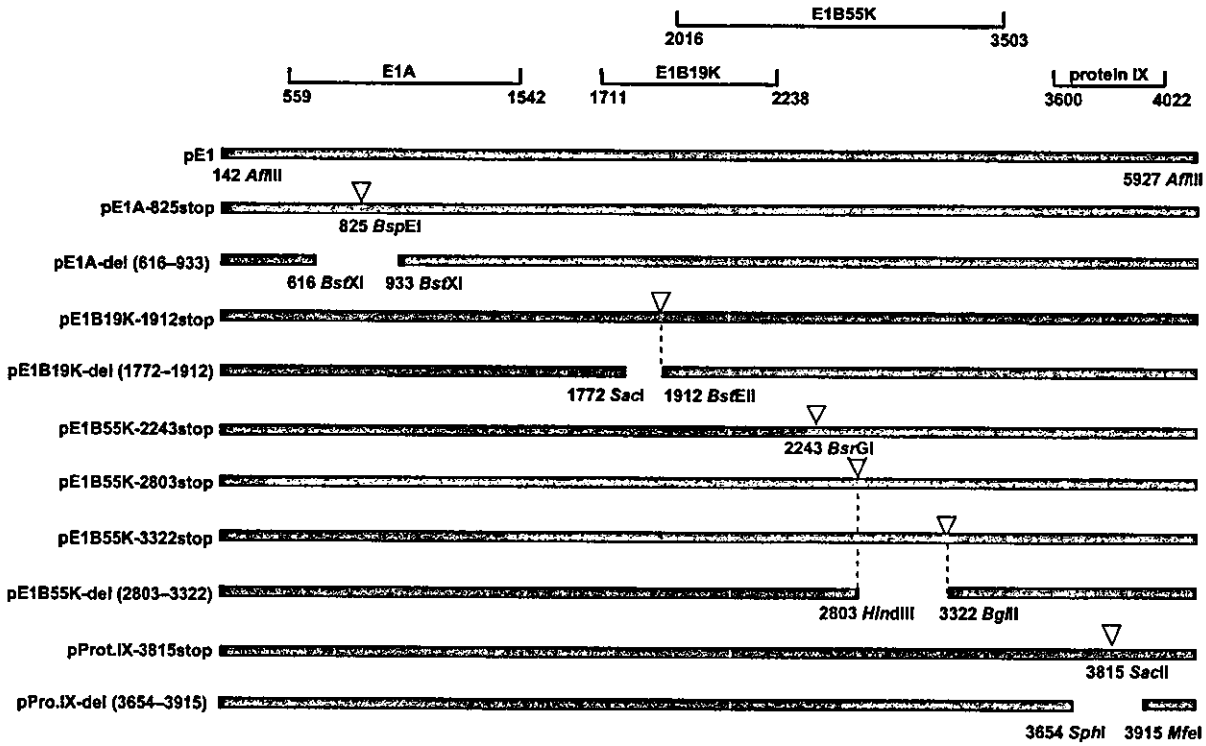

Fig. 1. Schematic representation of plasmids harbouring adenoviral E1 mutants used in this study. A 5·8 kb DNA fragment of adenovirus type 2 was cloned into the *Afl*III site of pBR322. pE1 encodes the entire E1 region, and the E1 mutant plasmids shown here were derived from it. The vertical flags mark the positions of inserted stop codons. The gaps in pE1A, pE1B19K, pE1B55K or pProt.IX constructs represent deletions.

pE1B55K-2803stop and pE1B55K-3322stop were made by the insertion of oligonucleotides into the *Bst*EII, *Bsr*GI, *Hin*dIII and *Bgl*II sites of pE1, respectively. pE1A-del (616–933) has a deletion of a 318 bp segment (positions 616–933 in Ad2). pE1B19K-del (1772–1912) and pE1B55K-del (2803–3322) have the same deletions as *dl337* (Pilder *et al.*, 1984) and *dl338* (Pilder *et al.*, 1986), respectively, used by Samulski & Shenk (1988) to examine E1 helper function for AAV2 production. Briefly, pE1B19K-del (1772–1912) lacks sequences between positions 1772 and 1912, and pE1B55K-del (2803–3322) lacks sequences between positions 2803 and 3322. pProt.IX-3815stop was constructed by the insertion of oligonucleotides into a *Sac*II site. pProt.IX-del (3654–3915) lacks a 262 bp segment (between positions 3654 and 3915 of Ad2).

The helper activities of the various E1 plasmids were assayed by cotransfecting them with a plasmid encoding both an AAV CMV*lacZ* vector and rep/cap (pW4389LacZ), and a plasmid encoding the adenovirus-2 VA RNA, E2A and E4 regions (Pladeno5), into KB or HeLa cells, and then quantifying *lacZ* vector production as described previously (Matsushita *et al.*, 1998). AAV vector was harvested 40 or 72 h after transfection and stocks were prepared by the freeze-thaw method. AAV vector production was quantified by titration of the vector stocks in 293 cells in the presence of adenovirus, followed by X-Gal staining and manual counting by light microscopy. For each experiment, all constructs were tested using triplicate production cultures, and all experiments were conducted at least three times, independently.

Elimination of the entire E1 region resulted in 2 (HeLa cells) to 3 log (KB cells) reduction in vector production relative to production in the presence of pE1, a plasmid encoding the entire E1 region ($P<0{\cdot}01$ by Student's *t*-test) (Fig. 2a, b). Disruption of the *E1A* genes, whether by truncation or deletion, caused 1 (HeLa cells) to 1·5 log (KB cells) reduction in vector production ($P<0{\cdot}01$). Truncations or deletions in the *E1B19K* gene also resulted in substantial reduction in vector production, 1 log in HeLa cells and greater than 2 logs in KB cells ($P<0{\cdot}01$). The lesser severity of the E1B19K mutant in HeLa cells, relative to KB cells, may be due to the relatively high level of Bcl-2 expression in HeLa cells (Liang *et al.*, 1995), or the human papilloma virus E6/E7 genes they harbour. The E6/E7 genes have been shown to facilitate some of the processes in AAV replication (Walz *et al.*, 1997). In most cases, disruption of the *E1B55K* and *protein IX* genes had a modest effect on vector production in either HeLa or KB cells. Two constructs, pE1B55K-2243stop and pProt.IX-3815stop showed fivefold reduction in vector yield in KB cells but little reduction in HeLa cells.

Our results differ substantially from those of Samulski & Shenk (1988) who examined the effect of E1B adenovirus mutants on AAV2 production, DNA replication, and mRNA and protein expression. This group found that an E1B19K adenovirus-2 mutant (*dl337*) mediated efficient AAV production from HeLa cells transfected with a plasmid encoding an AAV wild-type provirus (pSM620) but that

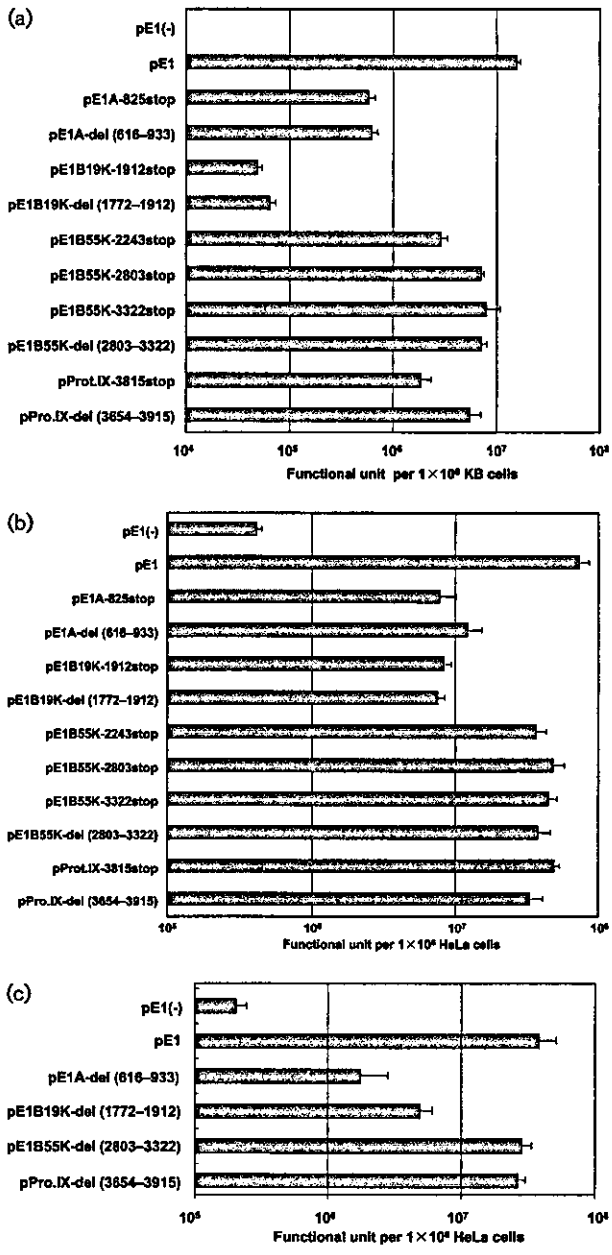

Fig. 2. Comparison of E1 mutant plasmids with respect to AAV helper function in KB (a) and HeLa cells (b) at 72 h after transfection, or in HeLa cells (c) at 40 h after the transfection. AAV *lacZ* vector was produced by the transfection of HeLa or KB cells with pW4389lacZ (encodes rep/cap and an AAV *lacZ* vector) and pladeno 5 (encodes the E2A, E4 and VA RNA regions), in the presence and absence of the indicated E1 plasmids. AAV vector production was assessed by titration of *lacZ* vector in 293 cells. pE1 (-) is identical to pBR322 without the expression cassette. Each bar represents the mean value obtained from triplicate cultures, and the error bar represents the standard deviation.

E1B55K (*dl338*) and E4orf6 (*dl355*) adenovirus mutants did not. AAV virion production was measured at a 40 h time point. The E1B55K and E4orf6 defects were caused by a delay in AAV mRNA accumulation that resulted in delays in viral DNA replication, capsid expression and ultimately virus production. AAV mRNA, DNA and capsid protein concentrations in cultures infected with E1B55K and E4orf6 mutants eventually reached levels seen in cultures infected by wild-type adenovirus but at longer time points, 72–96 h for adenovirus mutants compared with 24–40 h for wild-type adenovirus.

An important difference between our study and that of Samulski & Shenk (1988) was the timing of AAV/AAV vector harvest, 40 h in our study versus 72 h in theirs. Therefore, we examined a subset of the E1 region plasmids in transfection experiments using the same 40 h time point for vector harvest (Fig. 2c). The results were essentially similar to those at the 72 h time point and still differed from those produced by the adenovirus mutants. This observed difference in helper gene requirement may be attributable to technical factors associated with using virus infection or DNA transfection. A possible explanation for the conclusions reached by Samulski & Shenk (1988) might be the differences in the growth rates of the adenovirus mutants tested. The E1B55k mutant, *dl338*, was reported to grow inefficiently (100-fold reduced relative to wild-type) in HeLa cells (Pilder *et al.*, 1986) while the E1B19K mutant, *dl337*, was reported to be less defective (about 10-fold reduced relative to wild-type) (Pilder *et al.*, 1984). The lag in AAV mRNA, DNA and virus production seen with the E1B55K mutant may be simply because of a slow growing helper virus, resulting in low copy numbers of all of the adenovirus helper genes, and may not be directly due to the lack of the mutated gene. The observation that E1B19K is apparently not required for adenovirus mediated AAV production is harder to explain. It is tempting to speculate that the transfection-based production system benefits from additional anti-apoptitic activity provided by E1B19K. If this is true, this requirement does not appear to be cell-type or transfection-reagent specific (calcium phosphate and polycation-based transfection reagents both show an E1B19K effect, data not shown), and may have something to do with the adenoviral helper gene dose or kinetics of expression. Other differences between the two methods of identifying AAV helper function include: transfection method, the packaging of AAV virus versus a vector, and the use of replicating helper (AAV) versus non-replicating plasmid helpers. Full resolution of these issues will require further experimentation.

The adenovirus *E1B19K* gene, and its cellular homologues Bcl-2 and Bcl-x_L, encode anti-apoptotic proteins that function by inhibiting proapoptotic Bcl-2 homologues, such as Bax and Bak, by forming inactive heterodimers with them. To determine whether other anti-apoptotic members of the Bcl-2 family could augment AAV vector production, plasmid vectors expressing the *E1B19K*, *Bcl-2* or *Bcl-x_L* gene

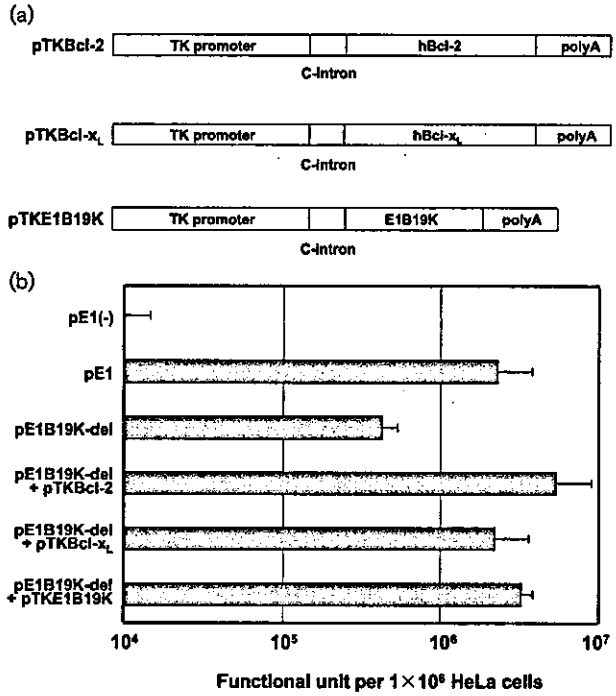

Fig. 3. (a) Schematic representation of Bcl-2, Bcl-x_L and E1B19K expression plasmids. TK promoter, HSV-*tk* promoter; C-intron, chimeric CMV/β-globin intron; polyA, SV40 late polyadenylation signal; hBcl-2, human Bcl-2 cDNA; hBcl-x_L, human Bcl-x_L cDNA; and E1B19K, adenovirus type 2 early region 1B 19 kDa protein gene. (b) Bcl-2 family members complement the vector production defect of an E1B19K mutant in HeLa cells. AAV *lacZ* vector was produced by the transfection of HeLa cells with pW4389lacZ (encodes rep/cap and an AAV *lacZ* vector), pladeno 5 (encodes the E2A, E4 and VA RNA regions), and pE1B19K-del (1772–1912), in the presence and absence of the indicated plasmids expressing Bcl-2 family genes, including E1B19K. AAV vector production was assessed by titration of *lacZ* vector in 293 cells. Each bar represents the mean value of triplicate cultures and the error bar represents the standard deviation.

products were tested for their ability to complement the vector production defect of the E1B19K deletion mutant, pE1B19K-del (1772–1912) (Fig. 3a). pTKPRMCS was assembled by the removal of a *Renilla* luciferase (R*luc*) reporter gene from pRL-TK (Promega) (between the *Nhe*I and *Xba*I sites) and insertion of a multiple cloning site (between the *Kpn*I and *Xba*I sites) from pBluescript II (Stratagene). pTK-Bcl-2 and pTK-Bcl-x_L were created by the insertion of human Bcl-2 and Bcl-x_L cDNA sequences, respectively, into pTKPRMCS. pTK-E1B19K was constructed by the insertion of the E1B19K fragment into pTKPRMCS. As shown in Fig. 3(b), plasmids expressing E1B19K, Bcl-2 or Bcl-x_L restored vector production of the E1B19K deletion mutant to levels equivalent to that produced by the wild-type pE1 plasmid. The use of the medium strength HSV-*tk* promoter to drive the expression

of the Bcl-2 homologues was essential for helper function. CMV-driven constructs produced low vector yields in a dominant fashion and caused a substantial increase in apoptosis (data not shown).

The fact that E1B19K mutants can be complemented by similarly anti-apoptotic cellular homologues such as Bcl-2 or Bcl-x_L suggests a common mechanism, the inhibition of Bak/Bax-mediated apoptosis. Interestingly, no increase in DNA ladder formation is seen in HeLa cells when transfected with E1B19K mutant plasmids relative to wild-type plasmids (data not shown). Consequently, the mechanism of vector production augmentation is not clear.

Current transfection-based AAV vector production methods are sufficient to commercially support gene therapy applications with large doses and small patient populations (e.g. haemophilia, other genetic diseases) or applications with small doses and large patient populations (e.g. Parkinson's disease). Applications with large doses and large patient populations (e.g. heart failure) will be a challenge for transfection-based production methods that scale linearly. Consequently, the construction of a producer cell line that is both helper virus-free, and suspension culture-adaptable, is of great interest. This is a formidable task since many of the viral helper proteins are toxic to the cell either alone (e.g. E2A) or in combination with other helper functions (e.g. E4orf6 and E1B55K, E1A and *rep*). The task is further complicated by genes such as E1B19K that must be expressed in a rather precise manner. Packaging cell lines containing inducible E1 genes, along with the E2a, VA and E4 regions, and an integrated AAV vector have been produced but were found to suffer from relatively low vector yield and substantial production instability (Qiao *et al.*, 2002). Both of these problems were likely due to, or exacerbated by, helper gene toxicity. Our data indicates that one source of toxicity, the inhibition of host mRNA nuclear export mediated by the E4orf6/E1B55K heterodimer, could be eliminated by not including the E1B55K gene in packaging cell lines.

Defining the minimum set of helper genes necessary for efficient vector production is the first step in creating suitable packaging cell lines for AAV vectors. Using our transfection-based assay, we define that set to be E1A, E1B19K, the VA RNAs, E2A and E4orf6 genes.

Acknowledgements

We thank Dr Lawrence H. Boise for providing the Bcl-x_L cDNA, and Dr Michael Lochrie and Dr Matthew Weitzman for manuscript review and helpful comments. We also thank Dr Tatsuya Nomoto and Ms Miyoko Mitsu for their encouragement and support. This work was supported in part by a Grant-in-Aid for Scientific Research on Priority Areas from the Ministry of Education, Science, Sports and Culture of Japan; a grant for Research on Human Genome and Gene Therapy from the Ministry of Health, Labour and Welfare of Japan; Core Research for Evolutional Science and Technology (CREST) of the Japan Science and Technology Corporation (JST); and a Jichi Medical School young investigator award.

References

Allen, J. M., Debelak, D. J., Reynolds, T. C. & Miller, A. D. (1997). Identification and elimination of replication-competent adeno-associated virus (AAV) that can arise by nonhomologous recombination during AAV vector production. *J Virol* **71**, 6816–6822.

Allen, J. M., Halbert, C. L. & Miller, A. D. (2000). Improved adeno-associated virus vector production with transfection of a single helper adenovirus gene, E4orf6. *Mol Ther* **1**, 88–95.

Atchinson, R. W., Casto, B. C. & Hammon, W. M. (1965). Adenovirus-associated defective virus particles. *Science* **149**, 754–756.

Buller, R. M., Janik, J. E., Sebring, E. D. & Rose, J. A. (1981). Herpes simplex virus types 1 and 2 completely help adenovirus-associated virus replication. *J Virol* **40**, 241–247.

Carter, B. J., Antoni, B. A. & Klessig, D. F. (1992). Adenovirus containing a deletion of the early region 2A gene allows growth of adeno-associated virus with decreased efficiency. *Virology* **191**, 473–476.

Chang, L. S. & Shenk, T. (1990). The adenovirus DNA-binding protein stimulates the rate of transcription directed by adenovirus and adeno-associated virus promoters. *J Virol* **64**, 2103–2109.

Gao, G., Qu, G., Burnham, M. S. & 7 other authors (2000). Purification of recombinant adeno-associated virus vectors by column chromatography and its performance *in vivo*. *Hum Gene Ther* **11**, 2079–2091.

Jooss, K., Yang, Y., Fisher, K. J. & Wilson, J. M. (1998). Transduction of dendritic cells by DNA viral vectors directs the immune response to transgene products in muscle fibers. *J Virol* **72**, 4212–4223.

Liang, X. H., Mungal, S., Ayscue, A., Meissner, J. D., Wodnicki, P., Hockenbery, D., Lockett, S. & Herman, B. (1995). Bcl-2 proto-oncogene expression in cervical carcinoma cell lines containing inactive p53. *J Cell Biochem* **57**, 509–521.

Lowe, S. W., Ruley, H. E., Jacks, T. & Housman, D. E. (1993). p53-dependent apoptosis modulates the cytotoxicity of anticancer agents. *Cell* **74**, 957–967.

Matsushita, T., Elliger, S., Elliger, C., Podsakoff, G., Villarreal, L., Kurtzman, G. J., Iwaki, Y. & Colosi, P. (1998). Adeno-associated virus vectors can be efficiently produced without helper virus. *Gene Ther* **5**, 938–945.

Pilder, S., Logan, J. & Shenk, T. (1984). Deletion of the gene encoding the adenovirus 5 early region 1b 21,000-molecular-weight polypeptide leads to degradation of viral and host cell DNA. *J Virol* **52**, 664–671.

Pilder, S., Moore, M., Logan, J. & Shenk, T. (1986). The adenovirus E1B-55K transforming polypeptide modulates transport or cytoplasmic stabilization of viral and host cell mRNAs. *Mol Cell Biol* **6**, 470–476.

Qiao, C., Li, J., Skold, A., Zhang, X. & Xiao, X. (2002). Feasibility of generating adeno-associated virus packaging cell lines containing inducible adenovirus genes. *J Virol* **76**, 1904–1913.

Querido, E., Marcellus, R. C., Lai, A., Charbonneau, R., Teodoro, J. G., Ketner, G. & Branton, P. E. (1997). Regulation of p53 levels by the E1B 55-kilodalton protein and E4orf6 in adenovirus-infected cells. *J Virol* **71**, 3788–3798.

Rabinowitz, J. E. & Samulski, J. (1998). Adeno-associated virus expression systems for gene transfer. *Curr Opin Biotechnol* **9**, 470–475.

Samulski, R. J. & Shenk, T. (1988). Adenovirus E1B 55-Mr polypeptide facilitates timely cytoplasmic accumulation of adeno-associated virus mRNAs. *J Virol* **62**, 206–210.

Schlehofer, J. R., Ehrbar, M. & zur Hausen, H. (1986). Vaccinia virus, herpes simplex virus, and carcinogens induce DNA amplification in a human cell line and support replication of a helpervirus dependent parvovirus. *Virology* **152**, 110–117.

Steegenga, W. T., Riteco, N., Jochemsen, A. G., Fallaux, F. J. & Bos, J. L. (1998). The large E1B protein together with the E4orf6 protein

target p53 for active degradation in adenovirus infected cells. *Oncogene* **16**, 349–357.

Tratschin, J. D., West, M. H., Sandbank, T. & Carter, B. J. (1984). A human parvovirus, adeno-associated virus, as a eucaryotic vector: transient expression and encapsidation of the procaryotic gene for chloramphenicol acetyltransferase. *Mol Cell Biol* **4**, 2072–2081.

Walz, C., Deprez, A., Dupressoir, T., Durst, M., Rabreau, M. & Schlehofer, J. R. (1997). Interaction of human papillomavirus type 16 and adeno-associated virus type 2 co-infecting human cervical epithelium. *J Gen Virol* **78**, 1441–1452.

Ward, P., Dean, F. B., O'Donnell, M. E. & Berns, K. I. (1998). Role of the adenovirus DNA-binding protein in *in vitro* adeno-associated virus DNA replication. *J Virol* **72**, 420–427.

West, M. H., Trempe, J. P., Tratschin, J. D. & Carter, B. J. (1987). Gene expression in adeno-associated virus vectors: the effects of chimeric mRNA structure, helper virus, and adenovirus VA1 RNA. *Virology* **160**, 38–47.

Xiao, X., Li, J. & Samulski, R. J. (1998). Production of high-titer recombinant adeno-associated virus vectors in the absence of helper adenovirus. *J Virol* **72**, 2224–2232.

Gene Therapy (2004) 11, 1081–1086

www.nature.com/gt

RESEARCH ARTICLE

Long-term correction of hyperphenylalaninemia by AAV-mediated gene transfer leads to behavioral recovery in phenylketonuria mice

S Mochizuki[1,2], H Mizukami[1], T Ogura[1], S Kure[3], A Ichinohe[3], K Kojima[3], Y Matsubara[3], E Kobayahi[4], T Okada[1], A Hoshika[2], K Ozawa[1,5] and A Kume[1]

[1]*Division of Genetic Therapeutics, Center for Molecular Medicine, Jichi Medical School, Tochigi, Japan;* [2]*Department of Pediatrics, Tokyo Medical University, Tokyo, Japan;* [3]*Department of Medical Genetics, Tohoku University Graduate School of Medicine, Sendai, Japan;* [4]*Division of Organ Replacement, Center for Molecular Medicine, Jichi Medical School, Tochigi, Japan; and* [5]*Division of Hematology, Department of Medicine, Jichi Medical School, Tochigi, Japan*

Classical phenylketonuria (PKU) is a metabolic disorder caused by a deficiency of the hepatic enzyme phenylalanine hydroxylase (PAH). If untreated, accumulation of phenylalanine will damage the developing brain of affected individuals, leading to severe mental retardation. Here, we show that a liver-directed PAH gene transfer brought about long-term correction of hyperphenylalaninemia and behavioral improvement in a mouse model of PKU. A recombinant adeno-associated virus (AAV) vector carrying the murine PAH cDNA was constructed and administered to PAH-deficient mice (strain PAH^{enu2}) via the portal vein. Within 2 weeks of treatment, the hyperphenylalaninemic phenotype improved and completely normalized in the animals treated with higher vector doses. The therapeutic effect persisted for 40 weeks in male mice, while serum phenylalanine concentrations in female animals gradually returned to pretreatment levels. Notably, this long-term correction of hyperphenylalaninemia was associated with a reversal of hypoactivity observed in PAH^{enu2} mice. While locomotory activity over 24 h and exploratory behavior were significantly decreased in untreated PAH^{enu2} mice compared with the age-matched controls, these indices were completely normalized in 12-month-old male PKU mice with lowered serum phenylalanine. These results demonstrate that AAV-mediated liver transduction ameliorated the PKU phenotype, including central nervous system dysfunctions.
Gene Therapy (2004) **11,** 1081–1086. doi:10.1038/sj.gt.3302262; Published online 1 April 2004

Keywords: *phenylketonuria; adeno-associated virus vector; hyperphenylalaninemia; behavioral recovery*

Introduction

Classical phenylketonuria (PKU; McKusick OMIM 261600) is an autosomal recessive disorder resulting from a deficiency of the liver enzyme phenylalanine hydroxylase (PAH; EC 1. 14.16.1).[1] PAH converts phenylalanine (Phe) to tyrosine with the aid of tetrahydrobiopterin (BH_4), and a deficiency of this enzyme causes accumulation of Phe and abnormal metabolites in the body fluids. If untreated, this condition irreversibly damages the central nervous system (CNS) of the patient, resulting in severe mental retardation. Conventional therapy for PKU consists of dietary restriction of Phe, which can prevent neuronal damage if initiated very early in life. However, the strict and complicated diet is often associated with poor compliance, particularly in adolescents and young adults. Premature termination of the diet leads to declined neuropsychological function, and noncompliance in pregnant women with PKU can produce devastating defects in the offspring referred to as 'maternal PKU syndrome'. A permanent cure is therefore awaited to liberate patients from dietary restrictions, and gene therapy is an attractive novel approach to this goal.

However, previous preclinical studies of PKU gene therapy have revealed that a long-term cure of PKU is a formidable task. Generally, recombinant retroviral vectors cannot deliver the normal PAH gene to the liver at sufficient levels to overcome hyperphenylalaninemia.[2,3] Adenoviral-mediated PAH gene transfer achieved a complete reduction of serum Phe in PKU animals, but the therapeutic effects did not persist and the vector was not effectively readministered due to immune responses against the virus.[4,5] On the other hand, adeno-associated virus (AAV) vectors comprise another class of gene delivery vehicles, which have been shown to stably transduce nondividing cells such as hepatocytes, muscle fibers and neurons.[6–8]

In this study, we evaluated a recombinant AAV vector carrying the PAH gene in a mouse model of PKU (PAH^{enu2} strain).[9–11] A missense mutation (F263S) in the PAH gene was introduced into BTBR mouse strain by chemical mutagenesis, resulting in a loss of enzyme activity. Consequently, the homozygous PAH^{enu2} mice

Correspondence: Dr A Kume, Division of Genetic Therapeutics, Center for Molecular Medicine, Jichi Medical School, 3311-1 Yakushiji, Minamikawachi, Tochigi 329-0498, Japan
Received 24 December 2003; accepted 11 February 2004; published online 1 April 2004

share many phenotypic characteristics with human PKU patients, such as profound hyperphenylalaninemia (>20 mg/dl; normal 1–2 mg/dl), behavioral disturbances and hypopigmentation. Previous work suggested that at least 10% of normal PAH activity would be required to prevent hyperphenylalaninemia in PKU mice.[4,5]

Results

Construction of the recombinant AAV vector

We first evaluated vectors derived from AAV serotypes 1 through 5. Recombinant AAV vectors containing the mouse erythropoietin (Epo) gene were infused into the mouse portal vein, and the serum Epo levels were determined. Among them, the AAV5-derived virion yielded the highest Epo concentration (unpublished results).[12,13] Next, we tested several promoters to drive the Epo gene in the context of AAV5. We found that the CAG promoter was the strongest in transgene expression in the liver (unpublished results).[14] This promoter consists of the human cytomegalovirus (CMV) immediate-early enhancer, the chicken β-actin promoter, and a chicken β-actin/rabbit β-globin composite intron.

Based on these results, we constructed an AAV vector as shown in Figure 1 (AAV5/CAG-mPAH). A recombinant AAV plasmid pAAV5/CAG-mPAH was comprised of the CAG promoter, the murine PAH cDNA and the SV40 late polyadenylation signal flanked by the AAV5 inverted terminal repeats (ITRs shown as hairpin loops in Figure 1). The vector DNA was then packaged into the AAV5 capsid through an adenovirus-free, transient transfection protocol.[15]

Correction of hyperphenylalaninemia

For liver-targeted gene transfer, the vector was injected into 5–7-week-old PAH^{enu2} mice via the portal vein. We injected male PKU mice with 3×10^{12} vector genomes (vg) ($n=3$), 1×10^{13} vg ($n=4$), 3×10^{13} vg ($n=3$) or 1×10^{14} vg ($n=3$) of AAV5/CAG-mPAH per animal. Female PKU mice were infused with 1×10^{13} vg ($n=4$), 3×10^{13} vg ($n=4$) or 1×10^{14} vg ($n=5$) per animal.

Serum Phe levels were determined prior to the infusion, biweekly until 12 weeks postinfusion, and every 4 weeks thereafter (Figure 2). Before gene transfer (week 0), all PAH-deficient mice showed profound hyperphenylalaninemia (33.7±3.4 mg/dl; range 29.3–43.5 mg/dl; $n=27$). The degree of hyperphenylalaninemia was not significantly different between males (33.2±2.6 mg/dl; $n=14$) and females (34.3±4.1 mg/dl; $n=13$). Figure 2a shows the kinetics of blood Phe in male PKU mice receiving different doses of AAV5/CAG-mPAH. A striking decrease in serum Phe was observed 2-4 weeks after gene transfer. With the lowest vector dose (3×10^{12} vg), serum Phe was only slightly lowered after 2 weeks (from 35.0±1.6 to 28.1±7.0 mg/dl; $P=0.18$ by paired *t*-test), but was significantly lowered after 4 weeks (15.6±6.9 mg/dl; $P=0.027$ by paired *t*-test). With higher vector doses (1×10^{13}, 3×10^{13} and 1×10^{14} vg), the serum Phe level was clearly lowered ($P=0.001$, 0.006 and 0.002 by paired *t*-test, respectively) to a therapeutic range (<10 mg/dl) in 2 weeks. At 4 weeks postinfusion, each cohort of male mice recorded the lowest serum Phe. In particular, it was completely normalized in the mice treated with 3×10^{13} vg (1.4±0.5 mg/dl) and 1×10^{14} vg (1.2±0.5 mg/dl) of AAV5/CAG-mPAH.

The reduced serum Phe levels were stably maintained for 40 weeks. Complete correction of hyperphenylalaninemia (<2 mg/dl) persisted in the mice treated with the highest vector dose (1×10^{14} vg), and the mice receiving

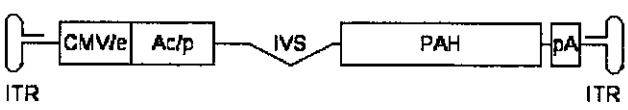

Figure 1 Structure of the AAV5/CAG-mPAH vector. The vector consisted of a CMV immediate-early enhancer (CMV/e), the chicken β-actin promoter (Ac/p), a chicken β-actin/rabbit β-globin composite intron (IVS), the 1.4 kb murine PAH cDNA (PAH) and the SV40 late polyadenylation signal (pA) flanked by the AAV5 inverted terminal repeats (ITRs shown as hairpin loops).

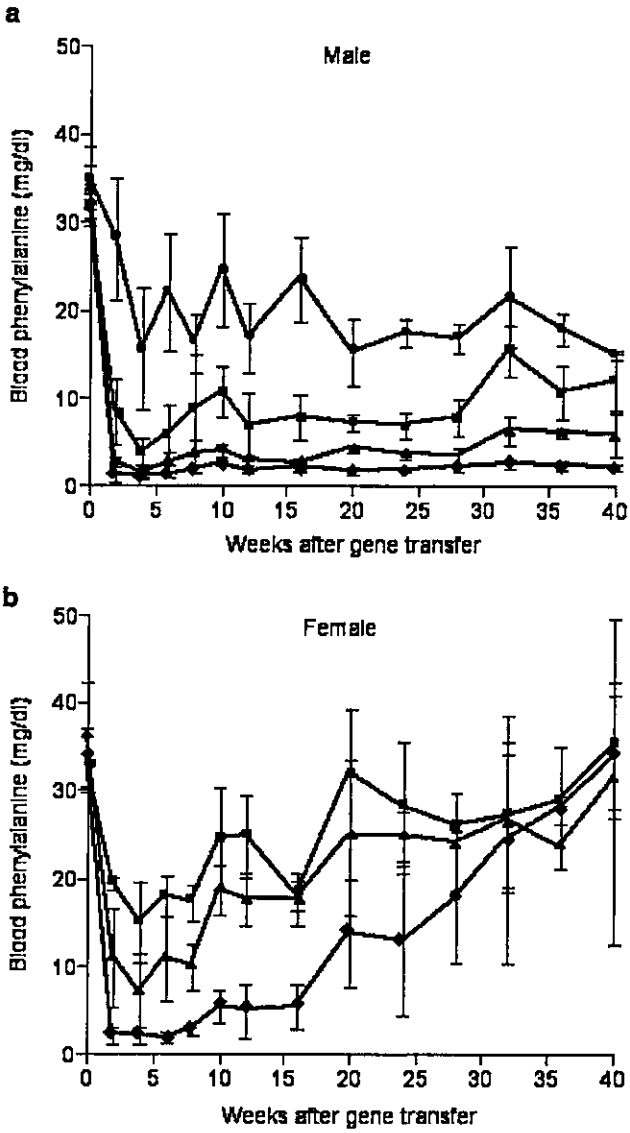

Figure 2 Persistence of the recombinant AAV-mediated correction of hyperphenylalaninemia in male (a) and female (b) PKU mice. Serum Phe concentration was determined prior to vector infusion (week 0) and periodically after gene transfer, and represented as the mean±s.d. for each treatment group. The applied vector dose was 3×10^{12} vg (circles), 1×10^{13} vg (squares), 3×10^{13} vg (triangles) or 1×10^{14} vg (diamonds) per animal.